ACCOUNTS of chemical research

Article

Cite This: Acc. Chem. Res. 2019, 52, 2491−2505

pubs.acs.org/accounts

Heteroatom-Doped Nanographenes with Structural Precision

Published as part of the Accounts of Chemical Research special issue "Advanced Molecular Nanocarbons".

Xiao-Ye Wang,*[,†,‡] Xuelin Yao,[‡] Akimitsu Narita,*[,‡,§] and Klaus Müllen*[,‡]

[†]State Key Laboratory of Elemento-Organic Chemistry, College of Chemistry, Nankai University, Tianjin 300071, China

[‡]Max Planck Institute for Polymer Research, Ackermannweg 10, 55128 Mainz, Germany

[§]Organic and Carbon Nanomaterials Unit, Okinawa Institute of Science and Technology Graduate University, Okinawa 904-0495, Japan

CONSPECTUS: Nanographenes, which are defined as nanoscale (1−100 nm) graphene cutouts, include quasi-one-dimensional graphene nanoribbons (GNRs) and quasi-zero-dimensional graphene quantum dots (GQDs). Polycyclic aromatic hydrocarbons (PAHs) larger than 1 nm can be viewed as GQDs with atomically precise molecular structures and can thus be termed nanographene molecules. As a result of quantum confinement, nanographenes are promising for next-generation semiconductor applications with finite band gaps, a significant advantage compared with gapless two-dimensional graphene. Similar to the atomic doping strategy in inorganic semiconductors, incorporation of heteroatoms into nanographenes is a viable way to tune their optical, electronic, catalytic, and magnetic properties. Such properties are highly dependent not only on the molecular size and edge structure but also on the heteroatom type, doping position, and concentration. Therefore, reliable synthetic methods are required to precisely control these structural features. In this regard, bottom-up organic synthesis provides an indispensable way to achieve structurally well-defined heteroatom-doped nanographenes.

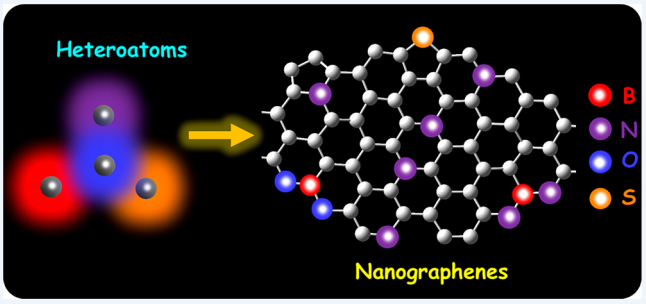

Polycyclic heteroaromatic compounds have attracted great attention of organic chemists for decades. Research in this direction has been further promoted by modern interest in supramolecular chemistry and organic electronics. The rise of graphene in the 21st century has endowed large polycyclic heteroaromatic compounds with a new role as model systems for heteroatom-doped graphene. Heteroatom-doped nanographene molecules are in their own right promising materials for photonic, optoelectronic, and spintronic applications because of the extended π conjugation. Despite the significant advances in polycyclic heteroaromatic compounds, heteroatom-doped nanographene molecules with sizes of over 1 nm and their relevant GNRs are still scarce.

In this Account, we describe the synthesis and properties of large heteroatom-doped nanographenes, mainly summarizing relevant advances in our group in the past decade. We first present several examples of heteroatom doping based on the prototypical nanographene molecule, i.e., hexa-*peri*-hexabenzocoronene (HBC), including nitrogen-doped HBC analogues by formal replacement of benzene with other heterocycles (e.g., aromatic pyrimidine and pyrrole and antiaromatic pyrazine) and sulfur-doped nanographene molecules via thiophene annulation. We then introduce heteroatom-doped zigzag edges and a variety of zigzag-edged nanographene molecules incorporating nitrogen, boron, and oxygen atoms. We finally summarize heteroatom-doped GNRs based on the success in the molecular cases. We hope that this Account will further stimulate the synthesis and applications of heteroatom-doped nanographenes with a combined effort from different disciplines.

1. INTRODUCTION

Since the isolation of single graphene layers by Geim and Novoselov,[1] graphene has opened up tremendous opportunities for materials science because of its extraordinary properties and broad applications.[2−5] In particular, the ultrahigh charge-carrier mobility of graphene is extremely appealing for electronic devices; however, the use of graphene as the active layer in field-effect transistors (FETs) is hindered by the lack of an electronic band gap because the devices cannot be switched off.[6] This disadvantage can be overcome by reduction in the dimensionality of graphene, generating quasi-zero-dimensional graphene quantum dots (GQDs) and quasi-one-dimensional graphene nanoribbons (GNRs) (Figure 1).[5,7] Because of quantum confinement, these nanoscale graphenes (nanographenes) are promising for next-generation semiconductor applications with finite band gaps.[8,9] The fabrication of nanographenes is often accomplished through top-down methods such as "cutting" of graphene and carbon nanotubes.[5] The applications of nanographenes, for example, in electronic devices, catalysis, bioimaging and sensing, have also been demonstrated.[8,10] However, the top-down approach cannot accurately control the size and edge structure, which are highly relevant to the physical and chemical properties of nanographenes. Therefore,

Received: June 18, 2019
Published: September 3, 2019

DOI: 10.1021/acs.accounts.9b00322
Acc. Chem. Res. 2019, 52, 2491−2505

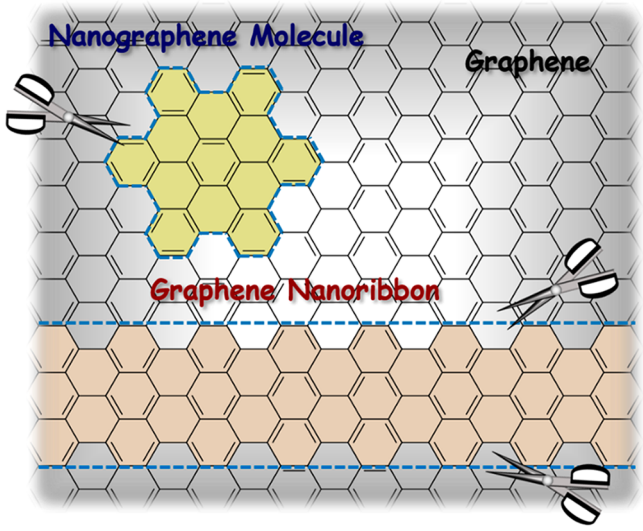

Figure 1. Schematic illustration of graphene and its nanoscale subunits (i.e., nanographenes), including nanographene molecules (atomically precise graphene quantum dots) and graphene nanoribbons.

control of the nanographene structure at the atomic level is required to achieve reliable structure−property correlations and desired functions.[5] This goal can be realized through bottom-up syntheses starting with molecular precursors, and this approach illustrates how organic chemists can contribute to the materials science of nanographenes, providing atomically precise GQDs (e.g., nanographene molecules) and GNRs.[11,12] The capability to precisely control nanographene structures further promotes the creation of emergent materials such as magnetic GNRs and topological insulators by rational molecular design.[13−15]

Atomic doping is a common strategy to tune the properties of inorganic materials, for instance, in silicon-based semiconductor industry: doping of silicon with group III or group V elements can achieve p-doped or n-doped semiconductors, respectively. The atomic doping strategy is also essential to nanographene materials through incorporation of heteroatoms into the graphenic carbon network, effectively modulating the electronic, magnetic, and catalytic properties.[16] Again, the bottom-up method is indispensable to achieve atomic precision not only in terms of the size and edge structure but also with regard to the heteroatom type, doping position, and concentration. This accuracy is an indispensable tool for controlling the physical properties and revealing structure−property relationships.[11,12] In addition, structurally well-defined heteroatom-doped nanographenes are intriguing semiconducting materials. The heteroatoms in the nanographene framework provide more opportunities for materials development (i) by modulating the band gap and thus the photophysical properties, (ii) by offering rich electrochemical activities, (iii) by installing coordinating sites for metals, and (iv) by stabilizing charges and spins in the carbon skeleton.[16] Nevertheless, large nanographene molecules and GNRs incorporating various heteroatoms (e.g., B,[17] N,[18,19] O,[20] S,[21] and P[22]) are still scarce.[16]

Our group has been working on the synthesis, characterization, and application of nanographenes during the past decades. In 1995 we reported the synthesis of alkyl-substituted hexa-*peri*-hexabenzocoronene (HBC) **1b**,[23] which has a diameter of over 1 nm and can thus be regarded as a nanographene molecule (Figure 2a).[5,7] Since this seminal work, we have synthesized various HBC derivatives and other larger nanographene molecules by means of a general synthetic strategy, namely, cyclodehydrogenation of polyphenylene precursors (e.g., hexaphenylbenzene **2**, Figure 2a) to afford planarized products.[24] The alkyl substituents not only impart solubility and solution processability to the disc-shaped nanographene molecules but also induce the formation of columnar liquid-crystalline mesophases (Figure 2b).[24] Charges can therefore be transported through the columnar $\pi-\pi$ stacking channel, which is a special concept for FETs and photovoltaic devices.[25−27] We have further extended the synthetic strategy to achieve atomically precise GNRs through conventional solution chemistry and modern on-surface syntheses.[28] These advances have been reviewed in our previous contributions.[5,7,11,12,24,28] In this Account, we focus on our works toward heteroatom-doped nanographenes, which have yet been comprehensively summarized. In the following, we will discuss the design, synthesis,

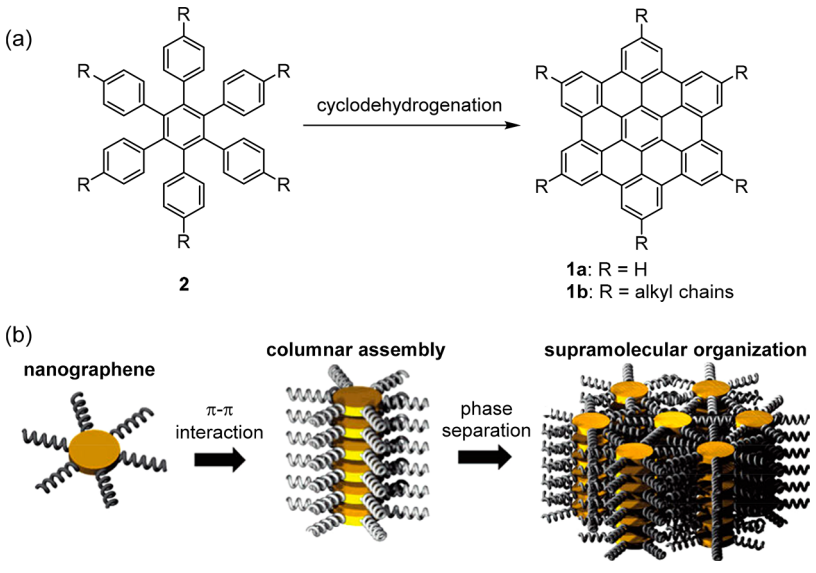

Figure 2. (a) Synthesis of HBCs from the corresponding hexaphenylbenzene precursors via cyclodehydrogenation. (b) Columnar self-assembly of disc-shaped nanographene molecules. Reproduced from ref 24. Copyright 2007 American Chemical Society.

DOI: 10.1021/acs.accounts.9b00322
Acc. Chem. Res. 2019, 52, 2491−2505

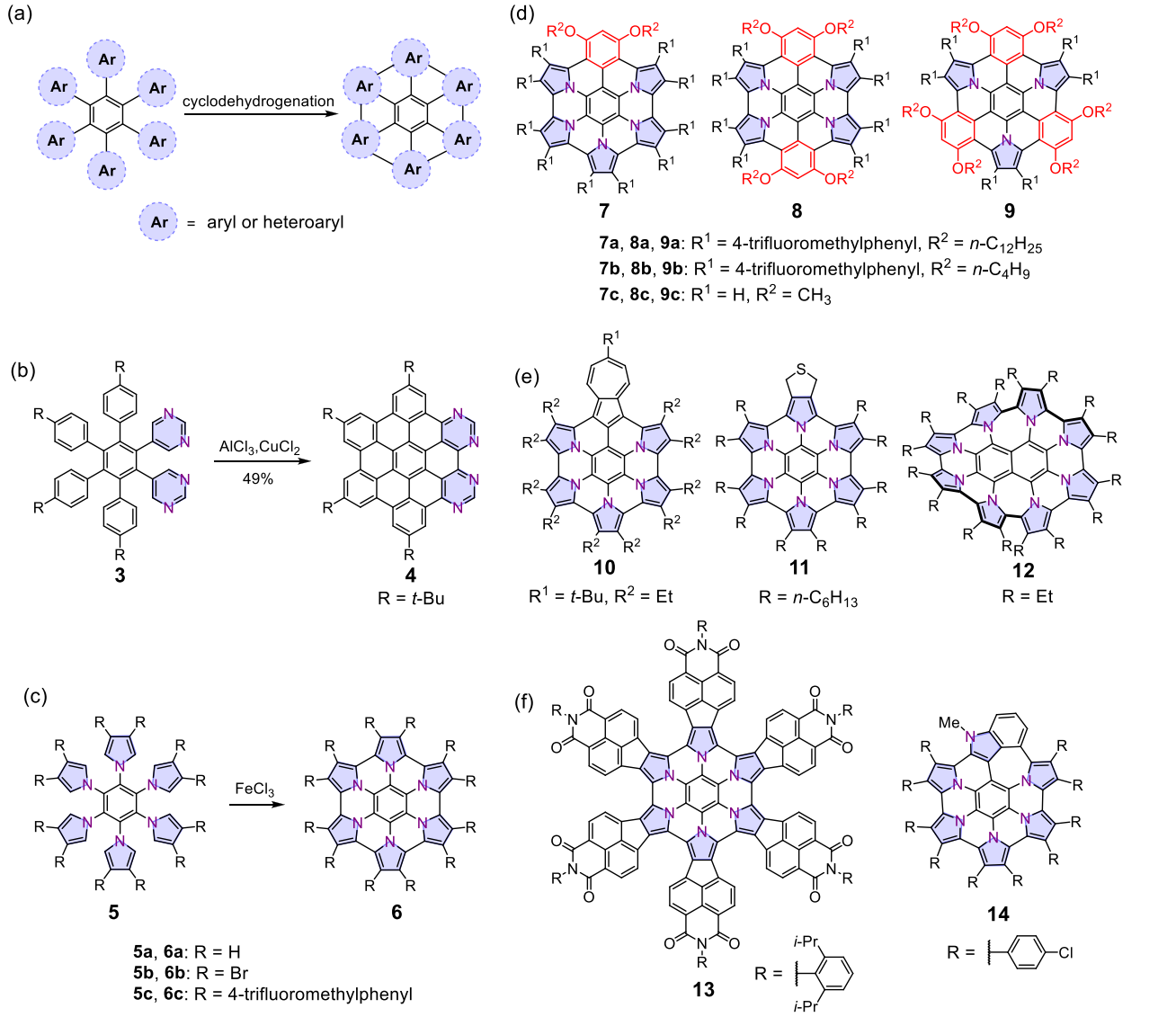

Figure 3. (a) General synthetic route to heteroatom-doped HBC analogues. (b) Synthesis of N-doped HBC **4** incorporating pyrimidine rings. (c) Synthesis of hexapyrrolohexaazacoronenes **6** incorporating pyrrole rings. (d) Several N-doped HBC analogues with a mixture of benzene and pyrrole rings. (e, f) Extensions of the hexapyrrolohexaazacoronene family, as exemplified by compounds **10**–**14**.

properties, and future opportunities of the research on heteroatom-doped nanographene molecules and GNRs.

2. FROM HBC TO HETEROATOM-DOPED HBC DERIVATIVES

2.1. Nitrogen-Doped Nanographene Molecules

Following the synthetic strategy of HBCs, it is easy to imagine the possibility of incorporating heteroatoms into the HBC skeleton by replacing the outer phenyl groups with other heteroaromatic rings in the hexaarylbenzene precursor (Figure 3a). Indeed, Draper et al. synthesized the first N-doped HBC **4** in 2002 through cyclodehydrogenation of the corresponding pyrimidine-substituted precursor **3** (Figure 3b).[29] The incorporation of pyrimidine rings endowed the nanographene molecule with electron-accepting properties compared with the parent HBC. Furthermore, the N atoms in the bay region served as a coordinating site with transition metals (e.g., Pd^{II} and Ru^{II}).[30] Not surprisingly, such metal complexes displayed profoundly changed absorption and emission features.

To develop electron-donating HBC analogues, in 2007 our group reported the synthesis and properties of hexapyrrolohexaazacoronenes **6** through oxidative cyclodehydrogenation of hexapyrrolylbenzene precursors **5** (Figure 3c).[31] The peripheral benzene rings were formally replaced with six pyrroles, providing a π skeleton isoelectronic to that of HBC. The interior nitrogens played an important role in stabilizing the oxidation states, and thereby, the dication of **6c** was generated by chemical oxidation and isolated under ambient conditions. Later on, together with Takase, Nishinaga, and co-workers, we extended the family of pyrrole-fused HBC analogues by incorporating a mixture of phenyl and pyrrolyl groups in the hexaarylbenzene precursors (Figure 3d).[32] This unique class of molecules has attracted great interest from other groups. For example, Takase, Uno, and co-workers made further modifications by changing the peripheral aryl moieties (compounds **10** and **11**) or by extending the benzene core to naphthalene (compound **12**) (Figure 3e).[33−35] Stępień et al. reported disc-shaped naphthalene monoimide-fused hexapyrrolohexaazacoronene **13** as well as an interesting

DOI: 10.1021/acs.accounts.9b00322
Acc. Chem. Res. 2019, 52, 2491−2505

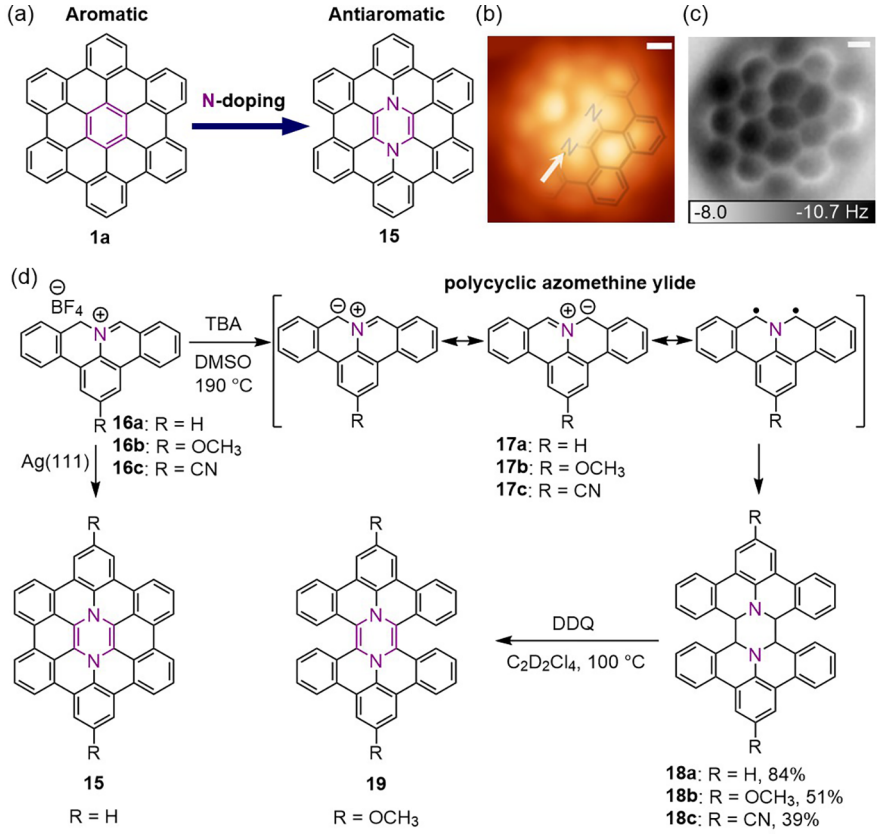

Figure 4. (a) Chemical structures of aromatic HBC **1a** and antiaromatic pyrazine-embedded HBC **15**. (b) STM and (c) nc-AFM images of **15**. Scale bars: 2 Å. A molecular model is partially superimposed on the STM image, and a white arrow pointing to the N atoms indicates the molecular symmetry axis. Reproduced with permission from ref 39. Published by Springer Nature. (d) Synthetic route to **15**. TBA, tri-*n*-butylamine; DMSO, dimethyl sulfoxide; DDQ, 2,3-dichloro-5,6-dicyano-1,4-benzoquinone.

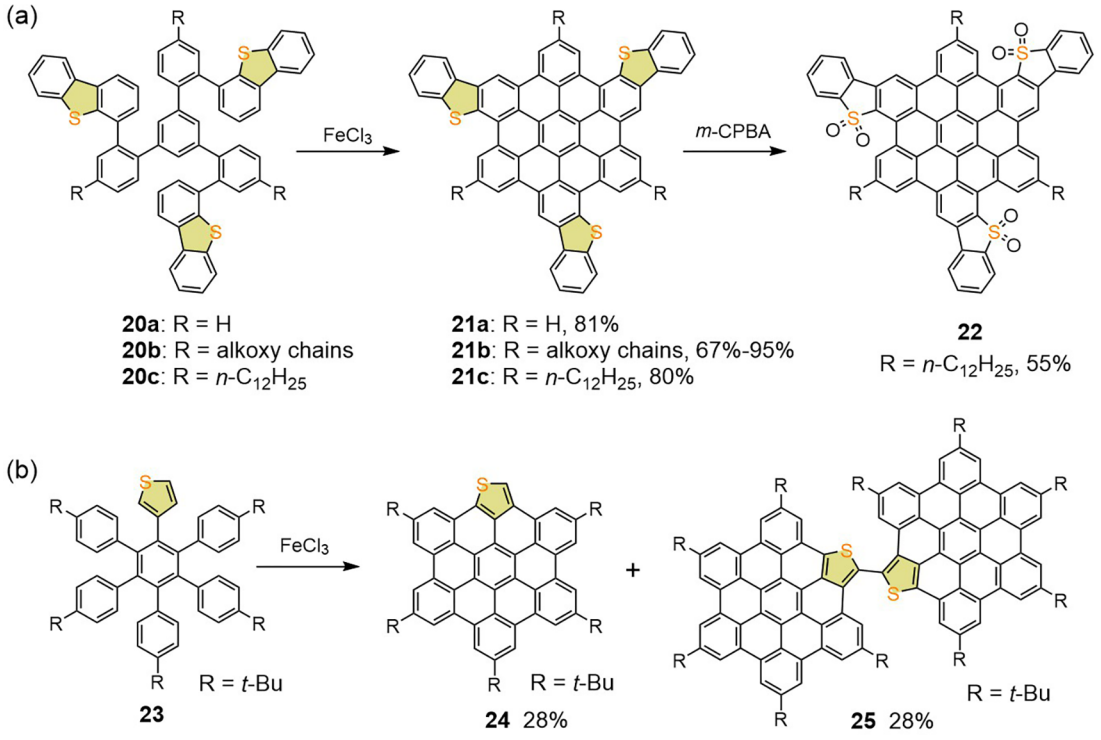

Figure 5. Syntheses of S-doped nanographene molecules. *m*-CPBA, *m*-chloroperoxybenzoic acid.

DOI: 10.1021/acs.accounts.9b00322
Acc. Chem. Res. 2019, 52, 2491−2505

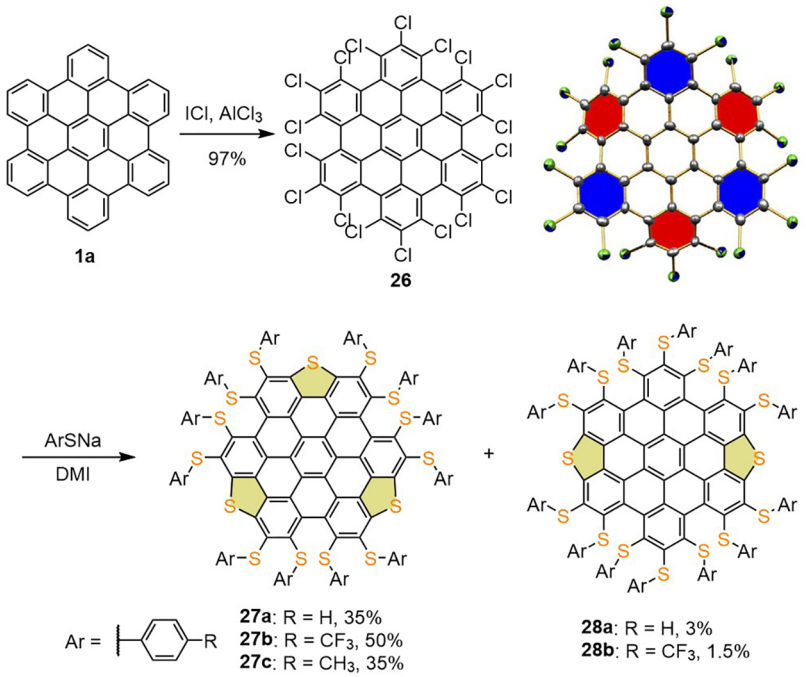

Figure 6. Synthesis of S-doped nanographene molecules **27** and **28** via postfunctionalization of perchlorinated HBC **26**. DMI, 1,3-dimethyl-2-imidazolidinone. The single-crystal structure of perchlorinated HBC **26** was reproduced with permission from ref 43. Copyright 2013 Macmillan Publishers Ltd.

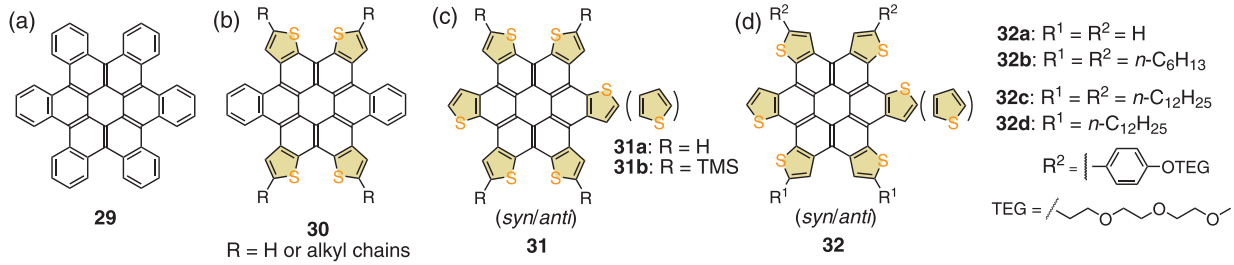

Figure 7. Chemical structures of (a, b) hexa-*cata*-hexabenzocoronene (**29**) and dibenzotetrathienocoronenes **30** as well as (c, d) hexathienocoronenes **31** and **32**.

derivative **14** containing five-, six-, and seven-membered rings, obtained from an indole-containing precursor (Figure 3f).[36,37]

As pyrimidine and pyrrole are both 6π aromatic heterocycles, incorporation of these rings into nanographene molecules does not change the aromatic nature because the number of π electrons is unchanged. From a chemistry perspective, we were interested in designing a new class of nanographene molecules involving antiaromatic rings that would lead to low energy gaps between the highest occupied molecular orbital (HOMO) and the lowest unoccupied molecular orbital (LUMO) as well as excellent redox properties.[38] In 2017, together with Auwärter, Barth, Palma, and co-workers, we conceived an azomethine ylide homocoupling strategy to achieve the synthesis of pyrazine-embedded HBC **15**, which possessed an 8π central ring through the introduction of a pyrazine core instead of a benzene core (Figure 4a).[39] After deprotonation of dibenzo-9*a*-azaphenalene salts **16**, polycyclic azomethine ylides (PAMYs) **17** were generated in situ with several existing resonance structures, including the zwitterionic and diradical forms (Figure 4d). The PAMYs were highly reactive and underwent dimerization in solution upon heating to afford "dimers" **18**. Oxidative dehydrogenation of **18b** in a sealed NMR tube under exclusion of air gave N-doped hexabenzoperylene **19**, but further cyclodehydrogenation in solution was unsuccessful. Nevertheless, the on-surface method enabled the synthesis of the fully fused N-doped HBC **15** through dimerization and concomitant cyclodehydrogenation on Ag(111) under ultrahigh vacuum (UHV) using dibenzo-9*a*-azaphenalene salt **16a** as the precursor. The chemical structure of **15** was unambiguously characterized by high-resolution scanning tunneling microscopy (STM) and noncontact atomic force microscopy (nc-AFM) with a CO-functionalized tip (Figure 4b,c). Density functional theory (DFT) calculations at the B3LYP/6-311G(d,p) level revealed a significantly narrowed HOMO−LUMO gap of **15** (2.06 eV) compared with that of the pristine HBC **1a** (3.57 eV), suggesting that the introduction of antiaromatic rings could be an effective way to tune the HOMO−LUMO gap and develop low-energy-gap nanographene materials.

2.2. Sulfur-Doped Nanographene Molecules

Incorporation of thiophene rings into the polyphenylene precursors results in S-doped nanographene molecules after cyclodehydrogenation. In 2007 we synthesized tribenzothiophene-fused HBC **21a** as the first example of S-doped nanographene molecules through cyclodehydrogenation of the C_3-symmetric precursor **20a** (Figure 5a).[40] Recently, the

DOI: 10.1021/acs.accounts.9b00322
Acc. Chem. Res. 2019, 52, 2491−2505

tribenzothiophene-fused HBC core of **21a** was derivatized by attaching alkoxy and alkyl chains (**21b** and **21c**) to ensure good solubility and to tune their HOMO and LUMO levels.[41] Remarkably, the electron-rich thiophene rings in the alkyl-substituted tribenzothiophene-fused HBC **21c** could be oxidized into electron-deficient thiophene-*S*,*S*-dioxide moieties, greatly lowering both the HOMO and LUMO levels by about 0.5 eV and representing an appealing feature of thiophene incorporation. In 2011, Draper et al. described another way of introducing thiophene rings in S-doped HBC analogue **24** (Figure 5b).[42] During the oxidative cyclodehydrogenation, dimerization of **24** was also observed via intermolecular oxidative coupling at the thiophene α-position.

Apart from the above-mentioned method through cyclodehydrogenation of suitable precursors to incorporate thiophene rings, we have also developed a postfunctionalization strategy to fuse thiophenes onto the HBC core based on edge-perchlorinated HBC **26**.[43] A thiolation reaction was performed to provide trithiophene-annelated HBCs **27** in 35−50% yield and dithiophene-annelated products **28** in 1.5−3% yield (Figure 6).[44] Furthermore, Tan, Zheng, and co-workers employed **27a** as hole-transporting material (HTM) in perovskite solar cells, providing the best efficiency of 12.8%, which could be improved to 14.0% through further device optimization.[45] Further studies indicated that **27a** endowed the devices with enhanced stability compared with the well-established HTM 2,2′,7,7′-tetrakis-[*N*,*N*-bis(4-methoxyphenyl)amino]-9,9′-spirobifluorene (Spiro-OMeTAD). In addition, together with Wu, Feng, and co-workers, we used nanographene molecule **27a** as a precursor to fabricate ultrathin S-doped graphene films, which were found to be applicable to ultrahigh-rate microsupercapacitors.[46]

Intrigued by the beautiful structure of contorted hexa-*cata*-hexabenzocoronene (**29**) (Figure 7a)[47] as well as its partially thiophene-substituted analogues such as dibenzotetrathienocoronenes **30** (Figure 7b) reported by Nuckolls et al.,[48] we synthesized two fully thiophene-fused coronenes, that is, hexathienocoronenes (HTCs) **31** and **32a−c** (Figure 7c,d).[49] HTCs **31** and **32a−c** exhibited almost identical absorption features and a highly electron-rich nature with higher HOMO levels compared with **30**. Single-crystal X-ray analysis revealed a columnar π-stacking structure of HTC **32b**. A discotic liquid-crystalline phase was observed for HTC **32c** with longer dodecyl chains. Together with Chen et al., we employed the backbone of HTC **32a** to form a gemini-type amphiphile by attaching hydrophobic and hydrophilic side chains on opposite sides of the aromatic core.[50] The obtained amphiphilic molecule **32d** self-assembled into nanofibers in solution. After chemical oxidation with nitrosonium tetrafluoroborate ($NOBF_4$), the nanofibers became electroconductive with a resistivity of 1.1 MΩ, which is lower than the value for the amphiphilic HBC nanotubes (2.5 MΩ).[51]

3. HETEROATOM DOPING ON THE ZIGZAG EDGES

The edge topologies of nanographene molecules, such as armchair and zigzag structures (Figure 8), are essential to their chemical and physical properties.[12] The majority of bottom-up-synthesized nanographene molecules have armchair edges, as represented by HBC and its derivatives. Although relatively rare, zigzag-edged nanographene molecules are particularly appealing, as they often have low HOMO−LUMO gaps and an open-shell ground state with long zigzag peripheries.[52] Despite the appealing characteristics of zigzag-edged nanographene molecules, their syntheses and characterizations are largely hampered by their instability under ambient conditions. On the one hand, replacement of the all-carbon zigzag edges with isostructural heteroatoms provides new access to stable nanographene molecules featuring zigzag architectures. On the other hand, heteroatom-doped zigzag edges are often theoretically considered as active sites in electrochemical catalysts for the oxygen reduction and hydrogen evolution reactions.[53,54] The synthesis of nanographene molecules having such edge structures can thus provide atomically precise models for investigating the electrocatalytic mechanism.

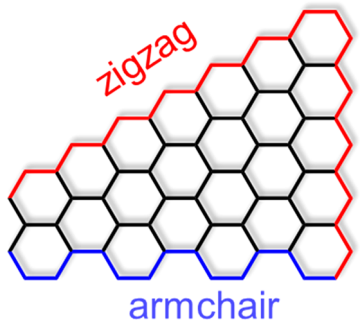

Figure 8. Schematic illustration of armchair and zigzag edge structures of nanographene molecules.

Inspired by the high performance of N-doped graphene-based materials for electrocatalysis, we synthesized dibenzo-9*a*-azaphenalene **35** as a model compound to study the catalytic activity of N-doped zigzag edges. Although we could not demonstrate a reasonable activity of **35** in electrocatalysis, we further achieved the synthesis of the linearly extended "dimer" **38** (Figure 9), indicating the potential of further extension toward the corresponding GNRs.[55] The PAMY unit in **35** was highly reactive, stemming from its diradical and zwitterionic resonance structures (Figure 4d). Therefore, compounds **35** and **38** were generated only under inert conditions by deprotonation of their charged precursors **34** and **37**. In addition, because of the extremely high chemical reactivity of the N-doped zigzag edges, the dibenzo-9*a*-azaphenalene-based PAMY offered a new entry to internally N-doped nanographene molecules through 1,3-dipolar cycloaddition with dipolarophiles.[56] This chemical reactivity was also independently exploited by Ito, Tokimaru, and Nozaki[57] and used for syntheses of azapentabenzocorannulene derivatives.[58,59]

We have also considered the incorporation of multiple heteroatoms to obtain stable heteroatom-doped zigzag edges and deeper insights into the effects of doping on the chemical and physical properties. Together with Zhang, Feng, and co-workers, we conceived nitrogen−boron−nitrogen (NBN)-doped zigzag peripheries based on 1,9-diaza-9*a*-boraphenalene as the next structural motif.[60] Both monomers **40** and the linearly fused "dimer" **45** were synthesized through electrophilic borylation (Figure 10). The NBN-doped zigzag edges exhibited high chemical stability, allowing for electrophilic bromination of **40b** and further modifications through cross-coupling reactions to give **42** (Figure 10a). Furthermore, chemical oxidation of monomers **40** led to σ dimers **43** connected at the positions *para* to the N atoms. To avoid such a dimerization reaction during oxidation, the active positions were protected by additional phenyl substituents (i.e., compound **42**). Clean single-electron oxidation of the NBN-doped zigzag peripheries to afford radical cation $\mathbf{42}^{\bullet+}$ was demonstrated by in situ spectroelectrochemis-

DOI: 10.1021/acs.accounts.9b00322
Acc. Chem. Res. 2019, 52, 2491−2505

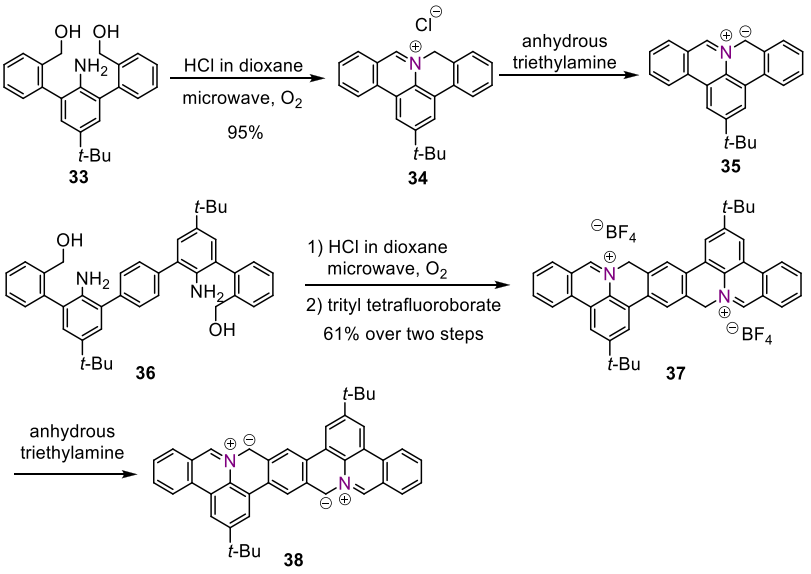

Figure 9. Synthesis of N-doped zigzag peripheries **35** and **38**.

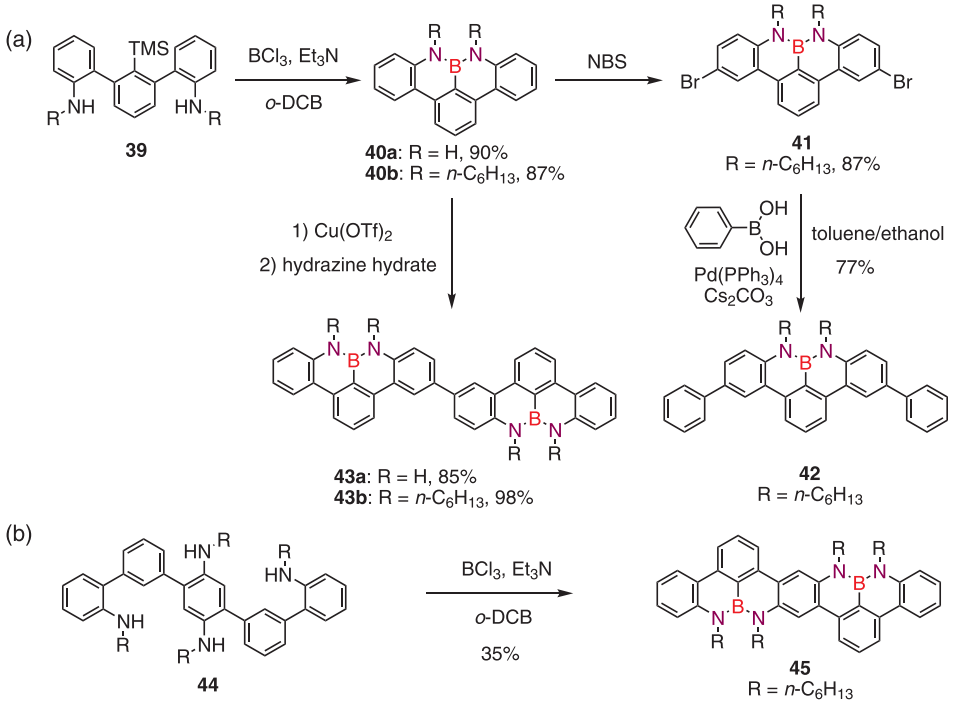

Figure 10. Synthesis of NBN-doped zigzag peripheries based on the 1,9-diaza-9*a*-boraphenalene motif. (a) Synthetic route to monomers **40** and further derivatizations. (b) Synthetic route to "dimer" **45**. NBS, *N*-bromosuccinimide; *o*-DCB, *o*-dichlorobenzene.

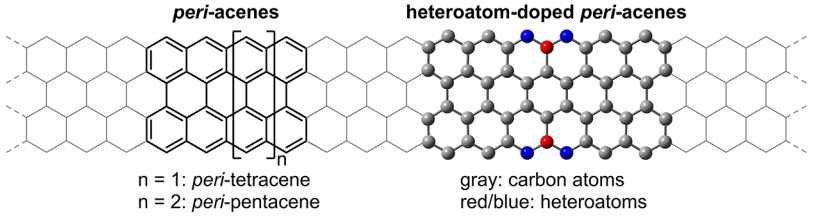

Figure 11. Schematic representations of *peri*-acenes and heteroatom-doped *peri*-acene-type nanographene molecules as a segment of full zigzag GNRs.

try, shedding light on the photophysical perperties of its isoelectronic dibenzophenalenyl radical.

In parallel to the studies on heteroatom-doped nanographene molecules, we also tried to tackle the syntheses of *peri*-acenes (e.g., *peri*-tetracene[61,62] and *peri*-pentacene[63]), which comprise two acenes laterally fused at all of the *peri* positions and can be viewed as segments of full zigzag GNRs (Figure 11). It was thus a logical extension to consider the synthesis of heteroatom-doped

DOI: 10.1021/acs.accounts.9b00322
Acc. Chem. Res. 2019, 52, 2491−2505

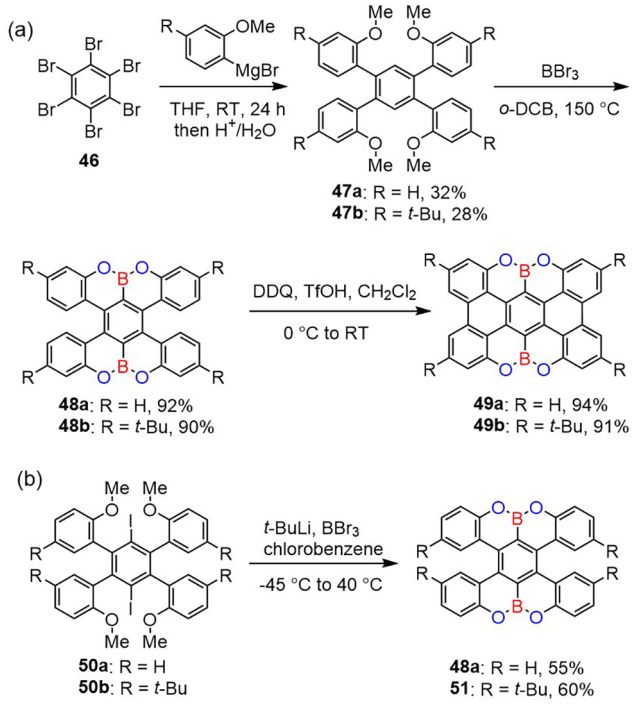

Figure 12. (a) Synthesis of OBO-doped *peri*-tetracenes **49**. (b) Another method to synthesize the uncyclized precursor **48a** and an isomer of **48b** with different substituent positions (compound **51**). TfOH, trifluoromethanesulfonic acid.

peri-acenes as the next targets. Our initial attempts to make NBN-doped *peri*-tetracene turned out to be challenging, and we are still working on different routes to synthesize it, but we were successful in installing oxygen−boron−oxygen (OBO) segments on the zigzag peripheries of *peri*-acenes. More specifically, we developed a tandem demethylation−borylation method to construct OBO-fused tetrabenzo[*a,f,j,o*]perylenes **48** by simple heating of precursors **47** with BBr_3 in *o*-dichlorobenzene (Figure 12a).[64] Further cyclodehydrogenation of **48** provided the first heteroatom-doped *peri*-tetracenes **49** in 2016, before the all-carbon *peri*-tetracenes were achieved in 2018.[65,66] The OBO-doped *peri*-tetracene exhibited excellent ambient stability, blue fluorescence, and a large HOMO−LUMO gap with a low-lying HOMO level compared with pristine *peri*-tetracene. The incorporation of OBO units drastically changed the properties of *peri*-tetracene, and therefore, isoelectronic heteroatom doping would be important to maintain the open-shell character of *peri*-tetracene while improving its stability for potential applications. It is noteworthy that Hatakeyama et al. independently reported compound **48a** obtaind by a different method (Figure 12b), in which a precursor containing two extra iodo groups was used to generate **48a** in 55% yield.[67] Our method gives higher yields (>90%) and is simpler since it is based on direct C−H borylation without the need for iodo groups in the precursor. It must be noted that Hatakeyama et al. also independently reported the use of the direct C−H borylation method to synthesize heteroatom-doped benzo[*fg*]-

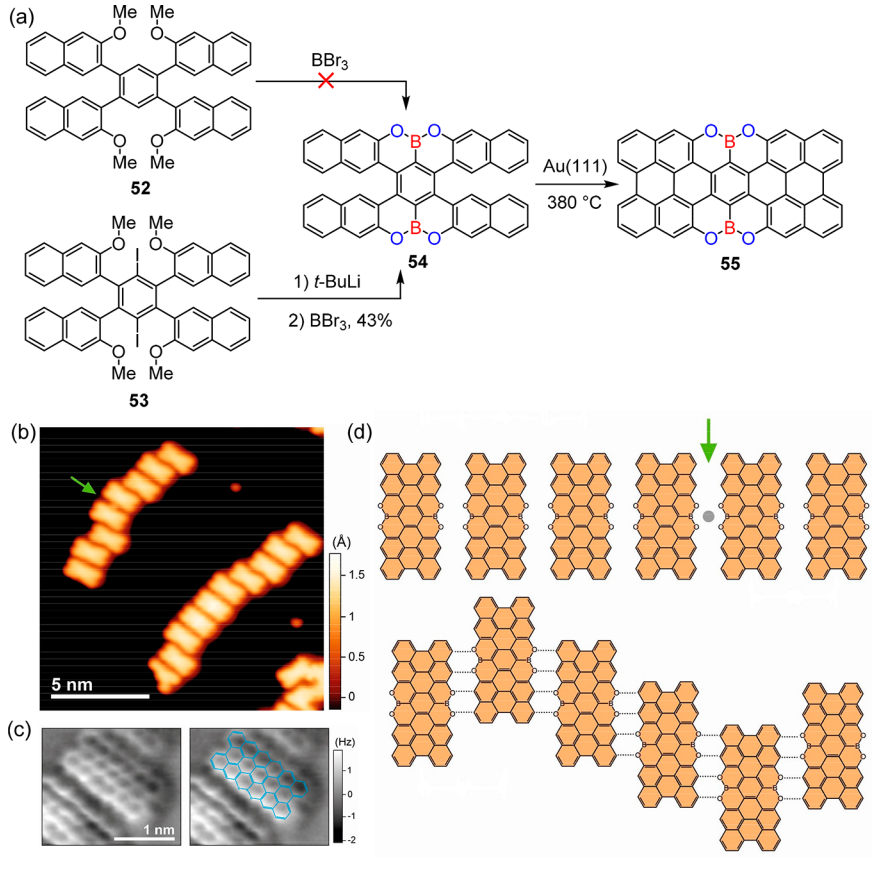

Figure 13. (a) Synthetic route to OBO-doped *peri*-hexacene **55**. (b) STM and (c) nc-AFM images of **55** on a Au(111) surface. (d) Schematic illustration of molecular assembly via metal coordination and O···H hydrogen bonding. Reproduced from ref 69. Copyright 2017 American Chemical Society.

DOI: 10.1021/acs.accounts.9b00322
Acc. Chem. Res. 2019, 52, 2491−2505

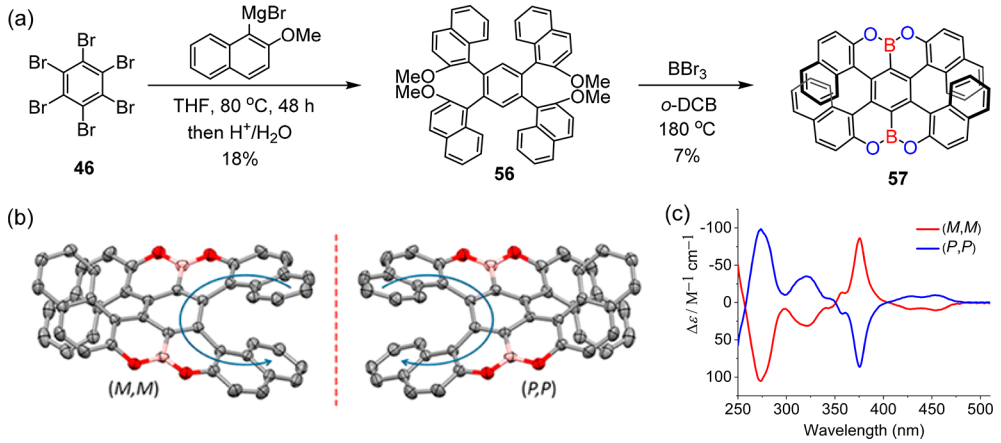

Figure 14. (a) Synthetic route to OBO-fused double [7]helicene **57**. (b) Single-crystal structures of the (*M*,*M*) and (*P*,*P*) isomers. (c) Circular dichroism spectra of the (*M*,*M*) and (*P*,*P*) isomers. Reproduced from ref 70. Copyright 2016 American Chemical Society.

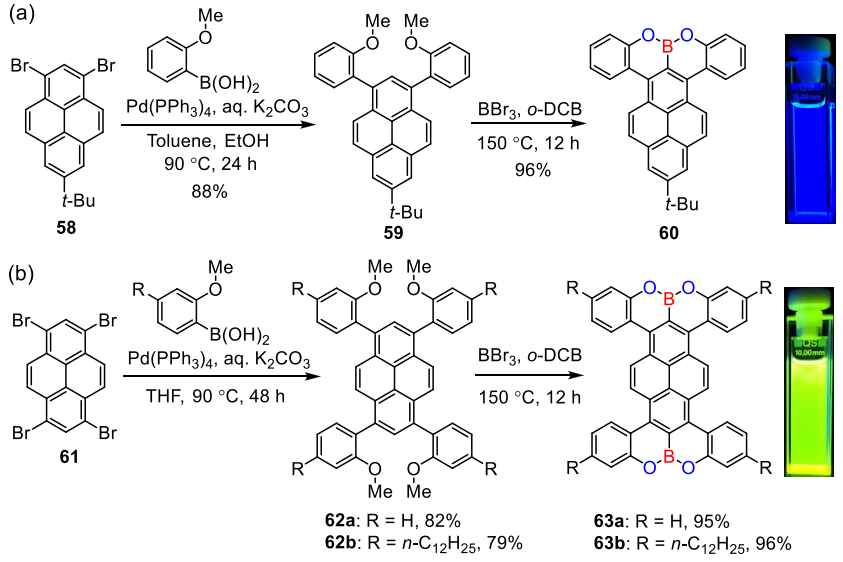

Figure 15. Synthetic routes to oxaborin-annelated pyrene derivatives **60** and **63** and their solutions in $CHCl_3$ under UV light (365 nm). Images were reproduced with permission from ref 71. Copyright 2018 Wiley-VCH Verlag GmbH & Co. KGaA, Weinheim.

tetracene structures with OBO, NBN, and SBS substitution on the zigzag peripheries.[68]

In our pursuit of longer *peri*-acene-type nanographene molecules, we synthesized OBO-doped *peri*-hexacene as the longest *peri*-acene analogue.[69] We first tried to furnish the OBO-fused precursor **54** by our tandem demethylation−borylation method from 1,2,4,5-tetrakis(3-methoxynaphthalen-2-yl)-benzene (**52**) (Figure 13a), but the reaction was not successful, probably because of the high reactivity of naphthalene *α*-positions during the electrophilic borylation. Therefore, we adopted Hatakeyama's method by introducing iodo groups on the central benzene to synthesize 1,4-diiodo-2,3,5,6-tetrakis(3-methoxynaphthalen-2-yl)benzene (**53**). After lithiation and reaction with BBr_3, the OBO-fused precursor **54** was obtained in 43% yield (Figure 13a). However, oxidative cyclodehydrogenation of **54** in solution did not provide the planarized product after attempts under different conditions. We thus employed on-surface synthesis in collaboration with Fasel et al. and achieved the OBO-doped perihexacene **55** on Au(111) by heating precursor **54** at 380 °C under UHV (Figure 13a). The structure of **55** was unambiguously characterized by STM and nc-AFM (Figure 13b,c). Furthermore, OBO-doped *peri*-hexacene **55** formed two kinds of 1D superstructures via intermolecular hydrogen bonding and metal coordination with the OBO segments on the zigzag edges (Figure 13b,d), demonstrating a potential edge-doping strategy for engineering self-assembled structures of graphene nanoarchitectures.

The OBO-fused precursor **54** featured a double [5]helicene substructure, which underwent a conformational change upon interactions with the surface.[69] On the other hand, in the crystal structure of double [5]helicene **48a**, we observed a pair of (*P*,*P*) and (*M*,*M*) enantiomers in one unit cell.[64] Hatakeyama et al. separated the enantiomers of such a double [5]helicene through the incorporation of bulky *tert*-butyl groups (compound **51**) to increase the isomerization energy barrier.[67] The interesting properties of double helicenes inspired us to further push the limit of double helicene synthesis and to explore their chiroptical properties. By adjusting the connectivity of the naphthalene rings, we synthesized the first double [7]helicene **57** (Figure 14a),[70] which is an isomer of the *π*-extended OBO-fused double [5]helicene **54**. Compound **57** was obtained in 7% yield through a tandem demethylation−borylation reaction of 1,2,4,5-tetrakis-(2-methoxynaphthalen-1-yl)benzene (**56**). The isolated yield is apparently lower than those of compounds **48** (over 90%),

DOI: 10.1021/acs.accounts.9b00322
Acc. Chem. Res. 2019, 52, 2491−2505

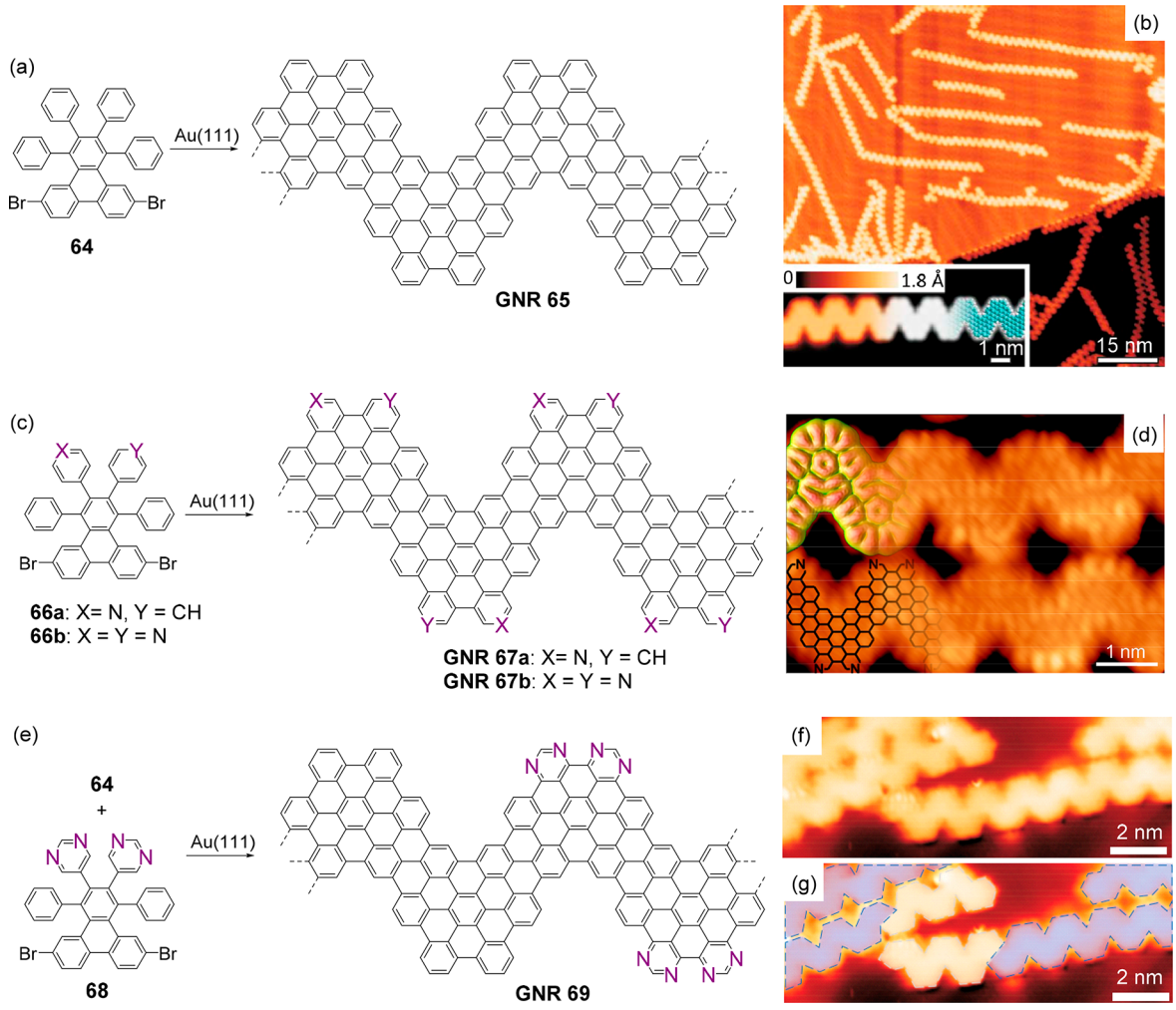

Figure 16. (a) Surface-assisted synthesis of chevron-type GNR **65**. (b) STM image of GNR **65** on a Au(111) surface. Reproduced with permission from ref 72. Copyright 2010 Macmillan Publishers Ltd. (c) Surface-assisted synthesis of N-doped chevron-type GNRs **67**. (d) High-resolution STM image of GNR **67b**, displaying a side-by-side alignment due to inter-ribbon N···H interactions. Reproduced with permission from ref 74. Copyright 2014 AIP Publishing LLC. (e) Surface-assisted synthesis of GNR heterojunction **69**. (f, g) STM images of GNR heterojuction **69**, with N-doped and pristine GNR segments highlighted in blue and light-gray dashed lines, respectively. Reproduced with permission from ref 75. Copyright 2014 Macmillan Publishers Ltd.

presumably because of the high strain built up during the ring closure. Single-crystal X-ray diffraction revealed substantial π overlap between the terminal benzene rings (Figure 14b). Compound **57** exhibited excellent chiral stability, which facilitated the optical resolution of the enantiomers by chiral HPLC. The separated (*P*,*P*) and (*M*,*M*) isomers displayed opposite responses in circular dichroism spectra (Figure 14c). The successful synthesis of the first double [7]helicene with OBO incorporation demonstrated the efficacy of the tandem demethylation–borylation method in the synthesis of even strained architectures, stimulating more efforts toward longer double helicenes and opening up a new avenue to chiral synthetic nanographenes.

To examine the scope of the tandem demethylation–borylation reaction, we tested the direct C–H borylation reactivity toward the chemically inert 2- and 7-positions of pyrene (Figure 15).[71] We found that the tandem reaction readily occurred under typical conditions, generating a new kind of oxaborin-annelated pyrene-based chromophores (**60** and **63**) in excellent yields (>95%). The singly annelated compound **60** displayed strong blue fluorescence (λ_{max} = 442 nm, Φ_F = 70%), whereas the doubly annelated product **63b** resembled perylene diimide (PDI) dyes in terms of bright green fluorescence (λ_{max} = 525 nm, Φ_F = 84%) and strong aggregation tendency in solution. The tandem demethylation–borylation reaction thus provided a new method for π extension of pyrene to obtain novel photonic and optoelectronic materials.

4. TOWARD HETEROATOM-DOPED GRAPHENE NANORIBBONS

The studies of the nanographene molecules have paved the way to heteroatom-doped GNRs by offering model cases. For example, when we established the surface-assisted synthesis of atomically precise GNRs together with Fasel et al. in 2010, we fabricated chevron-type GNR **65** from 6,11-dibromo-1,2,3,4-tetraphenyltriphenylene precursor **64** (Figure 16a,b).[72] The chevron-type GNR comprises HBC units that are fused side by side. Therefore, considering the many heteroatom-doped HBC analogues as described previously, one could easily imagine synthesizing heteroatom-doped chevron-type GNRs by modifying the triphenylene-based molecular precursors. Among the various possibilities, N doping is particularly interesting, as it can

DOI: 10.1021/acs.accounts.9b00322
Acc. Chem. Res. 2019, 52, 2491–2505

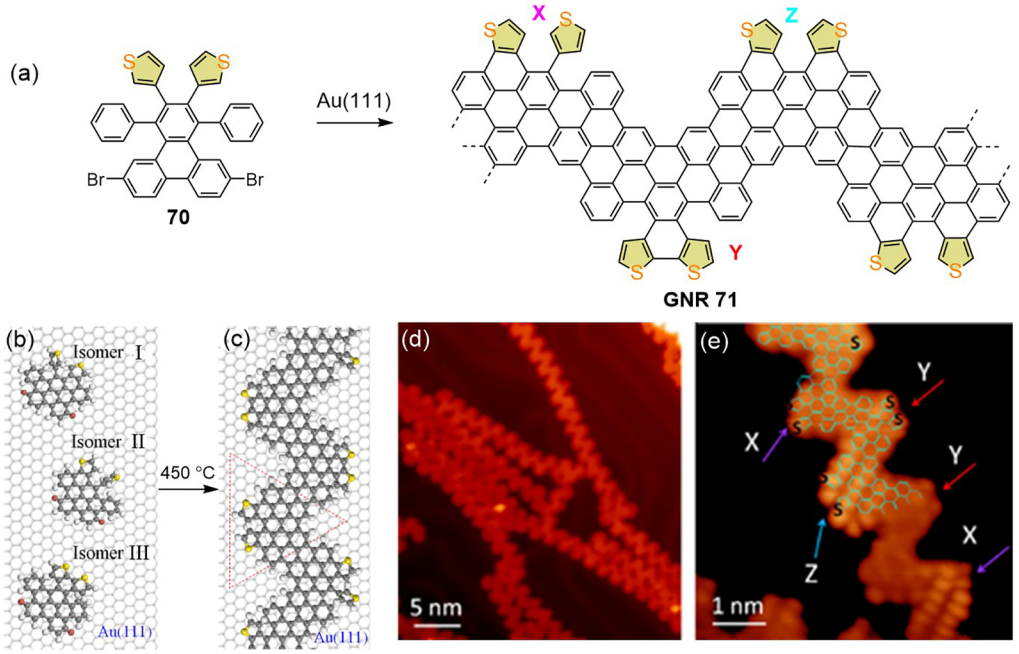

Figure 17. (a) Surface-assisted synthesis of S-doped GNR **71**. (b) Distinct isomers of **70** due to restriction of thienyl group rotation on Au(111). (c) Schematic illustration of GNR **71** on Au(111). (d) Large-area STM image of GNR **71**. (e) High-resolution STM image of GNR **71** with an overlaid chemical structure. Reproduced with permission from ref 76. Copyright 2017 Tsinghua University Press and Springer-Verlag GmbH Germany.

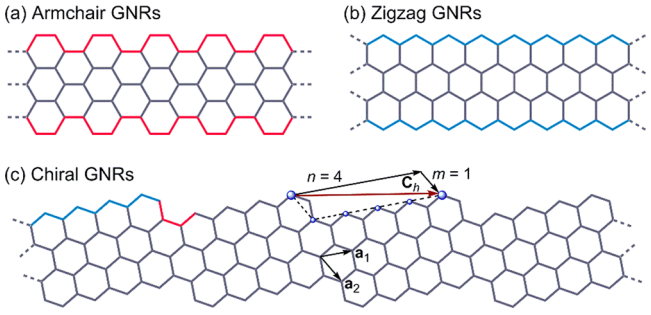

Figure 18. Schematic representation of (a) armchair GNRs, (b) zigzag GNRs, and (c) chiral GNRs. The edge configuration of chiral GNRs in (c) is defined by the translation vector $\mathbf{C}_h$, described as $\mathbf{C}_h = n\mathbf{a}_1 + m\mathbf{a}_2 = (n, m)$, where $\mathbf{a}_1$ and $\mathbf{a}_2$ represent the unit vectors of the graphene lattice. Reproduced from ref 78. Copyright 2018 American Chemical Society.

effectively lower the valence and conduction bands to afford n-type semiconductors. In 2013, Bronner, Hecht, Tegeder, and co-workers synthesized N-doped chevron-type GNRs **67** by replacing one or two phenyl rings with 4-pyridinyl groups in the monomers (Figure 16c).[73] Compared with the pristine chevron-type GNR **65**, the introduction of N atoms simultaneously lowered the valence and conduction bands, leaving the band gaps nearly unchanged. In 2014, together with Du, Gao, and co-workers, our group reported N-doped GNR **67b** fabricated on Au(111) under UHV and investigated its structure by high-resolution STM.[74] Different from its all-carbon counterpart **65**, the N-doped GNR **67b** exhibited a side-by-side alignment due to the inter-ribbon N···H interactions (Figure 16d). In the same year, together with Fasel et al., we reported the on-surface synthesis of GNR heterojunction **69** comprising alternating pristine and N-doped GNR segments (Figure 16e–g).[75] The incorporation of N atoms was accomplished by replacing two phenyl groups with 5-pyrimidinyl rings in the triphenylene-based precursor to give monomer **68**. The resulting GNR heterojunction **69** displayed a band offset of about 0.5 eV, representing the first GNR-based p–n junction and indicating great potential for future applications in nanoelectronics.

N-doping of GNRs in the form of pyridine and pyrimidine rings lowers the energies of the valence and conduction bands, whereas the band gap is nearly unaffected because the lone pair of N atoms is not conjugated with the GNR π system. In this regard, S doping in the form of thiophene incorporation is supposed to involve the lone pair in the π conjugation of GNRs and thus can effectively modulate the electronic structures and band gaps. Recently, together with Du, Gao, and co-workers, our group described the on-surface synthesis of S-doped GNR **71** by employing 6,11-dibromo-1,4-diphenyl-2,3-bis(thien-3-yl)-triphenylene (**70**) as the monomer (Figure 17a), that is, by replacing two phenyl rings with 3-thienyl groups in the typical triphenylene-based monomer.[76] Different from the N-doped chevron-type GNRs, the rotation of the single bonds connecting thienyl rings and the triphenylene core led to different isomers when the precursor was deposited on the Au(111) surface (Figure 17b). After polymerization and cyclodehydrogenation at 450 °C, different S-doped GNR segments were obtained (Figure 17c–e), giving rise to a sequence of tunable band gaps (1.28–1.78 eV), as confirmed by experimental STM and scanning tunneling spectroscopy (STS) as well as theoretical calculations. Through molecular engineering of the triphenylene-based monomers, Fischer et al. further achieved heteroatom-doped chevron-type GNRs with trigonal-planar S-, N-, and O-dopant atoms.[77]

As we had developed heteroatom-doped zigzag-edged nanographene molecules, we subsequently aimed at synthesizing GNRs with heteroatom-doped zigzag edge topologies. During the past years, although armchair GNRs have been extensively investigated,[79] zigzag GNRs have very rarely been achieved (Figure 18).[13] Chiral GNRs with a mixture of armchair

DOI: 10.1021/acs.accounts.9b00322
Acc. Chem. Res. 2019, 52, 2491–2505

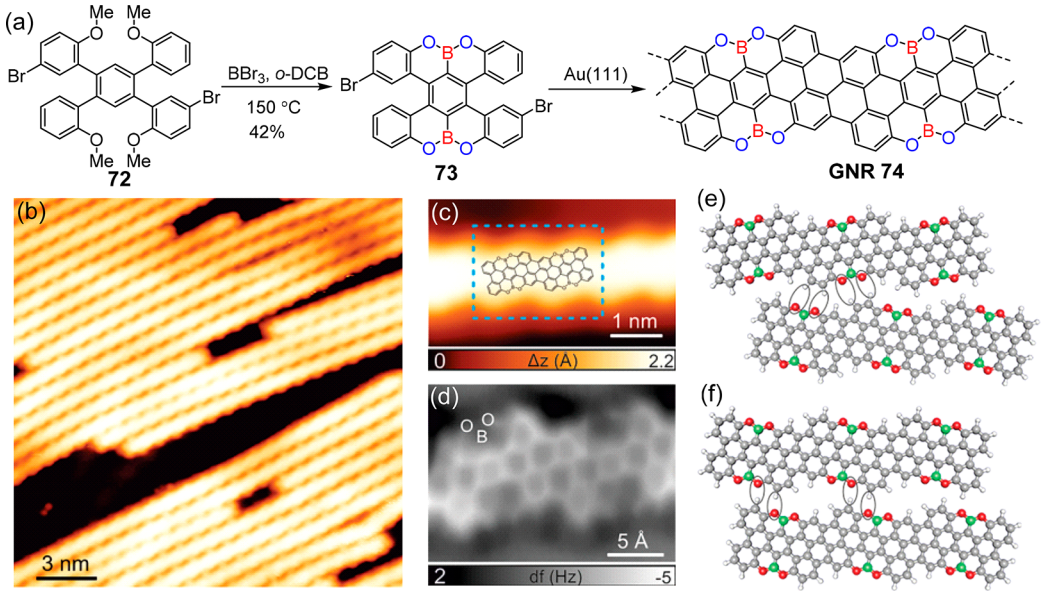

Figure 19. (a) Surface-assisted synthesis of OBO-doped (4,1)-GNR **74**. (b) Large-area STM image and (c) high-resolution STM image of GNR **74** on Au(111). (d) nc-AFM image of GNR **74**. (e, f) Theoretically calculated models of inter-ribbon interactions for heterochiral and homochiral assemblies of GNR **74**, respectively. Reproduced from ref 78. Copyright 2018 American Chemical Society.

and zigzag edges have also attracted great attention, but the bottom-up-synthesized structures have been limited only to (3,1)-GNRs (for the definition of the chiral index, see Figure 18) obtained from 9,9′-bianthracene-based monomers,[80] calling for further variations of the chiral edge configurations.

In 2018, together with Fasel et al., we reported the surface-assisted synthesis of the first heteroatom-doped chiral (4,1)-GNR **74** from the rationally designed monomer 6,16-dibromo-9,10,19,20-tetraoxa-9a,19a-diboratetrabenzo[*a*,*f*,*j*,*o*]perylene (**73**) containing both boron and oxygen (Figure 19a). It should be noted that bottom-up-synthesized GNRs with multiple heteroatom substitution are still scarce.[81] Monomer **73** was synthesized through tandem demethylation−borylation of 1,4-bis(5′-bromo-2′-methoxyphenyl)-2,5-bis(2′-methoxyphenyl)-benzene (**72**) bearing two bromo groups. The structure of the chiral GNRs was characterized by STM and nc-AFM (Figure 19b−d) as well as Raman spectroscopy. STS studies and theoretical calculations revealed a larger band gap of the OBO-doped (4,1)-GNRs compared with the pristine (4,1)-GNRs. As a result of the OBO units on the edges, lateral assembly of the chiral GNRs was observed, achieving aligned GNR arrays with different homochiral and heterochiral inter-ribbon assembly modes (Figure 19e,f). The first OBO-doped GNRs suggested that the OBO structures on the edges facilitated lateral alignment of GNRs, which would be of importance for future GNR-based devices.

5. CONCLUSIONS AND OUTLOOK

We have summarized our works on heteroatom-doped nanographene molecules and GNRs during the past decade. On the basis of the prototypical nanographene molecule HBC, we have explored N doping through the incorporation of aromatic pyrrole and antiaromatic pyrazine rings. We have also developed a series of thiophene-annelated HBC derivatives as S-doped nanographene molecules. These results have promoted heteroatom doping as a powerful method for modulating the energy levels, band gaps, aromaticity, electron densities, and magnetic properties of nanographene molecules. Moreover, being aware of the importance of zigzag-edged nanographene molecules, we have explored heteroatom doping on zigzag edge structures, including generation of the PAMY as well as NBN and OBO incorporation. In particular, the OBO-doped compounds are easy to synthesize and are stable under ambient conditions, thereby representing a new class of nanographene molecules, including stable *peri*-tetracene and *peri*-hexacene analogues displaying intermolecular self-assembly tendency on the surface and double [7]helicene with high chiral stability as well as new pyrene-based chromophores. All of these achievements in nanographene molecules have paved the way to heteroatom-doped GNRs, such as N-doped and S-doped chevron-type GNRs with tunable band gaps and OBO-doped chiral (4,1)-GNRs with lateral alignment.

Nanocarbon science has attracted increasing interest in recent years, giving rise to a variety of carbon nanostructures. The incorporation of heteroatoms into the carbon frameworks provides a number of new opportunities to fine-tune the molecular properties. Certainly this process defines grand challenges in synthesis, thereby requesting the development of new and efficient synthetic methods. Convincing cases have been demonstrated in the PAMY chemistry and the tandem demethylation−borylation reaction, both of which have opened up new avenues to various heteroatom-doped nanographenes. Furthermore, the synthesis of heteroatom-doped GNRs is lagging behind that of nanographene molecules. There is much room to explore new structures such as pyrrole- and pyrazine-incorporated GNRs and heteroatom-doped full zigzag GNRs. In any case, close collaborations among chemists, physicists, and engineers are required to realize the applications of GNRs in future nanoelectronic and spintronic devices.

AUTHOR INFORMATION

Corresponding Authors

*E-mail: xiaoye.wang@nankai.edu.cn.
*E-mail: narita@mpip-mainz.mpg.de.
*E-mail: muellen@mpip-mainz.mpg.de.

DOI: 10.1021/acs.accounts.9b00322
Acc. Chem. Res. 2019, 52, 2491−2505

ORCID

Xiao-Ye Wang: 0000-0003-3540-0277
Akimitsu Narita: 0000-0002-3625-522X
Klaus Müllen: 0000-0001-6630-8786

Notes

The authors declare no competing financial interest.

Biographies

Xiao-Ye Wang received his Bachelor's degree from Nankai University in 2009 and obtained his Ph.D. degree from Peking University in 2014 under the supervision of Prof. Jian Pei. From 2014 to 2019 he was a postdoctoral researcher and a Humboldt Fellow in the group of Prof. Klaus Müllen at the Max Planck Institute for Polymer Research (MPIP) in Mainz, Germany. He has been a professor at Nankai University since 2019. His research focuses on organic conjugated materials, nanocarbon molecules, and their optoelectronic applications.

Xuelin Yao received his Bachelor's degree in 2012 and his Master's degree in 2015 from Sichuan University. Since 2015 he has been a member of the group of Prof. Klaus Müllen at MPIP as a Ph.D. candidate. His current research focuses on the synthesis of nanographene molecules and graphene nanoribbons with different edge topologies.

Akimitsu Narita received his Bachelor's degree in 2008 and his Master's degree in 2010 at The University of Tokyo under the supervision of Prof. Eiichi Nakamura. In 2014 he obtained his Ph.D. in the group of Prof. Klaus Müllen at MPIP. Beginning in 2014, he became a project leader at MPIP. He is also an adjunct assistant professor at Okinawa Institute of Science and Technology Graduate School since 2018. His current research focuses on the bottom-up synthesis of functional nanographene molecules and graphene nanoribbons.

Klaus Müllen studied chemistry at the University of Cologne and received his Ph.D. from the University of Basel in 1971. After postdoctoral research and his habilitation at ETH Zurich, he joined the University of Cologne as a Professor in 1979 and moved to the University of Mainz in 1984. From 1989 to 2016 he was Director of the Synthetic Chemistry Department at MPIP. Since 2016 he has been the leader of an emeritus group at MPIP. His current research focuses on synthetic macromolecular chemistry, supramolecular chemistry, and materials science.

■ ACKNOWLEDGMENTS

We thank all of our distinguished collaborators and group members who enabled the achievements described in this Account. Financial support from the Max Planck Society, the Alexander von Humboldt Foundation, and the China Scholarship Council is gratefully acknowledged.

■ REFERENCES

(1) Novoselov, K. S.; Geim, A. K.; Morozov, S. V.; Jiang, D.; Zhang, Y.; Dubonos, S. V.; Grigorieva, I. V.; Firsov, A. A. Electric Field Effect in Atomically Thin Carbon Films. *Science* **2004**, *306*, 666−669.

(2) Geim, A. K.; Novoselov, K. S. The Rise of Graphene. *Nat. Mater.* **2007**, *6*, 183−191.

(3) Geim, A. K. Graphene: Status and Prospects. *Science* **2009**, *324*, 1530−1534.

(4) Novoselov, K. S.; Fal'ko, V. I.; Colombo, L.; Gellert, P. R.; Schwab, M. G.; Kim, K. A Roadmap for Graphene. *Nature* **2012**, *490*, 192−200.

(5) Wang, X.-Y.; Narita, A.; Müllen, K. Precision Synthesis versus Bulk-Scale Fabrication of Graphenes. *Nat. Rev. Chem.* **2018**, *2*, 0100.

(6) Schwierz, F. Graphene Transistors. *Nat. Nanotechnol.* **2010**, *5*, 487−496.

(7) Chen, L.; Hernandez, Y.; Feng, X.; Müllen, K. From Nanographene and Graphene Nanoribbons to Graphene Sheets: Chemical Synthesis. *Angew. Chem., Int. Ed.* **2012**, *51*, 7640−7654.

(8) Li, X.; Wang, X.; Zhang, L.; Lee, S.; Dai, H. Chemically Derived, Ultrasmooth Graphene Nanoribbon Semiconductors. *Science* **2008**, *319*, 1229−1232.

(9) Ponomarenko, L. A.; Schedin, F.; Katsnelson, M. I.; Yang, R.; Hill, E. W.; Novoselov, K. S.; Geim, A. K. Chaotic Dirac Billiard in Graphene Quantum Dots. *Science* **2008**, *320*, 356−358.

(10) Shen, J.; Zhu, Y.; Yang, X.; Li, C. Graphene Quantum Dots: Emergent Nanolights for Bioimaging, Sensors, Catalysis and Photovoltaic Devices. *Chem. Commun.* **2012**, *48*, 3686−3699.

(11) Narita, A.; Wang, X.-Y.; Feng, X.; Müllen, K. New Advances in Nanographene Chemistry. *Chem. Soc. Rev.* **2015**, *44*, 6616−6643.

(12) Wang, X.-Y.; Yao, X.; Müllen, K. Polycyclic Aromatic Hydrocarbons in the Graphene Era. *Sci. China: Chem.* **2019**, *62*, 1099−1144.

(13) Ruffieux, P.; Wang, S.; Yang, B.; Sánchez-Sánchez, C.; Liu, J.; Dienel, T.; Talirz, L.; Shinde, P.; Pignedoli, C. A.; Passerone, D.; Dumslaff, T.; Feng, X.; Müllen, K.; Fasel, R. On-Surface Synthesis of Graphene Nanoribbons with Zigzag Edge Topology. *Nature* **2016**, *531*, 489−492.

(14) Gröning, O.; Wang, S.; Yao, X.; Pignedoli, C. A.; Borin Barin, G.; Daniels, C.; Cupo, A.; Meunier, V.; Feng, X.; Narita, A.; Müllen, K.; Ruffieux, P.; Fasel, R. Engineering of Robust Topological Quantum Phases in Graphene Nanoribbons. *Nature* **2018**, *560*, 209−213.

(15) Rizzo, D. J.; Veber, G.; Cao, T.; Bronner, C.; Chen, T.; Zhao, F.; Rodriguez, H.; Louie, S. G.; Crommie, M. F.; Fischer, F. R. Topological Band Engineering of Graphene Nanoribbons. *Nature* **2018**, *560*, 204−208.

(16) Stępień, M.; Gońka, E.; Żyła, M.; Sprutta, N. Heterocyclic Nanographenes and Other Polycyclic Heteroaromatic Compounds: Synthetic Routes, Properties, and Applications. *Chem. Rev.* **2017**, *117*, 3479−3716.

(17) Dou, C.; Saito, S.; Matsuo, K.; Hisaki, I.; Yamaguchi, S. A Boron-Containing PAH as a Substructure of Boron-Doped Graphene. *Angew. Chem., Int. Ed.* **2012**, *51*, 12206−12210.

(18) Hahn, U.; Maisonhaute, E.; Nierengarten, J.-F. Twisted N-Doped Nano-Graphenes: Synthesis, Characterization, and Resolution. *Angew. Chem., Int. Ed.* **2018**, *57*, 10635−10639.

(19) Mishra, S.; Krzeszewski, M.; Pignedoli, C. A.; Ruffieux, P.; Fasel, R.; Gryko, D. T. On-Surface Synthesis of a Nitrogen-Embedded Buckybowl with Inverse Stone−Thrower−Wales Topology. *Nat. Commun.* **2018**, *9*, 1714.

(20) Berezin, A.; Biot, N.; Battisti, T.; Bonifazi, D. Oxygen-Doped Zig-Zag Molecular Ribbons. *Angew. Chem., Int. Ed.* **2018**, *57*, 8942−8946.

(21) Nguyen, G. D.; Toma, F. M.; Cao, T.; Pedramrazi, Z.; Chen, C.; Rizzo, D. J.; Joshi, T.; Bronner, C.; Chen, Y.-C.; Favaro, M.; Louie, S. G.; Fischer, F. R.; Crommie, M. F. Bottom-Up Synthesis of N = 13 Sulfur-Doped Graphene Nanoribbons. *J. Phys. Chem. C* **2016**, *120*, 2684−2687.

(22) Bouit, P.-A.; Escande, A.; Szűcs, R.; Szieberth, D.; Lescop, C.; Nyulászi, L.; Hissler, M.; Réau, R. Dibenzophosphapentaphenes: Exploiting P Chemistry for Gap Fine-Tuning and Coordination-Driven Assembly of Planar Polycyclic Aromatic Hydrocarbons. *J. Am. Chem. Soc.* **2012**, *134*, 6524−6527.

(23) Stabel, A.; Herwig, P.; Müllen, K.; Rabe, J. P. Diodelike Current−Voltage Curves for a Single Molecule−Tunneling Spectroscopy with Submolecular Resolution of an Alkylated, Peri-Condensed Hexabenzocoronene. *Angew. Chem., Int. Ed. Engl.* **1995**, *34*, 1609−1611.

(24) Wu, J.; Pisula, W.; Müllen, K. Graphenes as Potential Material for Electronics. *Chem. Rev.* **2007**, *107*, 718−747.

(25) van de Craats, A. M.; Stutzmann, N.; Bunk, O.; Nielsen, M. M.; Watson, M.; Müllen, K.; Chanzy, H. D.; Sirringhaus, H.; Friend, R. H. Meso-Epitaxial Solution-Growth of Self-Organizing Discotic Liquid-Crystalline Semiconductors. *Adv. Mater.* **2003**, *15*, 495−499.

(26) Pisula, W.; Menon, A.; Stepputat, M.; Lieberwirth, I.; Kolb, U.; Tracz, A.; Sirringhaus, H.; Pakula, T.; Müllen, K. A Zone-Casting Technique for Device Fabrication of Field-Effect Transistors Based on

DOI: 10.1021/acs.accounts.9b00322
Acc. Chem. Res. 2019, 52, 2491−2505

Discotic Hexa-Peri-Hexabenzocoronene. *Adv. Mater.* **2005**, *17*, 684−689.
(27) Schmidt-Mende, L.; Fechtenkötter, A.; Müllen, K.; Moons, E.; Friend, R. H.; MacKenzie, J. D. Self-Organized Discotic Liquid Crystals for High-Efficiency Organic Photovoltaics. *Science* **2001**, *293*, 1119−1122.
(28) Narita, A.; Chen, Z.; Chen, Q.; Müllen, K. Solution and On-Surface Synthesis of Structurally Defined Graphene Nanoribbons as a New Family of Semiconductors. *Chem. Sci.* **2019**, *10*, 964−975.
(29) Draper, S. M.; Gregg, D. J.; Madathil, R. Heterosuperbenzenes: A New Family of Nitrogen-Functionalized, Graphitic Molecules. *J. Am. Chem. Soc.* **2002**, *124*, 3486−3487.
(30) Draper, S. M.; Gregg, D. J.; Schofield, E. R.; Browne, W. R.; Duati, M.; Vos, J. G.; Passaniti, P. Complexed Nitrogen Heterosuperbenzene: The Coordinating Properties of a Remarkable Ligand. *J. Am. Chem. Soc.* **2004**, *126*, 8694−8701.
(31) Takase, M.; Enkelmann, V.; Sebastiani, D.; Baumgarten, M.; Müllen, K. Annularly Fused Hexapyrrolohexaazacoronenes: An Extended π System with Multiple Interior Nitrogen Atoms Displays Stable Oxidation States. *Angew. Chem., Int. Ed.* **2007**, *46*, 5524−5527.
(32) Takase, M.; Narita, T.; Fujita, W.; Asano, M. S.; Nishinaga, T.; Benten, H.; Yoza, K.; Müllen, K. Pyrrole-Fused Azacoronene Family: The Influence of Replacement with Dialkoxybenzenes on the Optical and Electronic Properties in Neutral and Oxidized States. *J. Am. Chem. Soc.* **2013**, *135*, 8031−8040.
(33) Sasaki, Y.; Takase, M.; Okujima, T.; Mori, S.; Uno, H. Synthesis and Redox Properties of Pyrrole- and Azulene-Fused Azacoronene. *Org. Lett.* **2019**, *21*, 1900−1903.
(34) Uno, H.; Ishiwata, M.; Muramatsu, K.; Takase, M.; Mori, S.; Okujima, T. Oxidation Behavior of 1,3-Dihydrothieno[3,4-*a*]HPHAC. *Bull. Chem. Soc. Jpn.* **2019**, *92*, 973−981.
(35) Oki, K.; Takase, M.; Mori, S.; Shiotari, A.; Sugimoto, Y.; Ohara, K.; Okujima, T.; Uno, H. Synthesis, Structures, and Properties of Core-Expanded Azacoronene Analogue: A Twisted π-System with Two N-Doped Heptagons. *J. Am. Chem. Soc.* **2018**, *140*, 10430−10434.
(36) Żyła-Karwowska, M.; Zhylitskaya, H.; Cybińska, J.; Lis, T.; Chmielewski, P. J.; Stępień, M. An Electron-Deficient Azacoronene Obtained by Radial π Extension. *Angew. Chem., Int. Ed.* **2016**, *55*, 14658−14662.
(37) Żyła, M.; Gońka, E.; Chmielewski, P. J.; Cybińska, J.; Stępień, M. Synthesis of a Peripherally Conjugated 5−6−7 Nanographene. *Chem. Sci.* **2016**, *7*, 286−294.
(38) Liu, J.; Ma, J.; Zhang, K.; Ravat, P.; Machata, P.; Avdoshenko, S.; Hennersdorf, F.; Komber, H.; Pisula, W.; Weigand, J. J.; Popov, A. A.; Berger, R.; Müllen, K.; Feng, X. π-Extended and Curved Antiaromatic Polycyclic Hydrocarbons. *J. Am. Chem. Soc.* **2017**, *139*, 7513−7521.
(39) Wang, X.-Y.; Richter, M.; He, Y.; Björk, J.; Riss, A.; Rajesh, R.; Garnica, M.; Hennersdorf, F.; Weigand, J. J.; Narita, A.; Berger, R.; Feng, X.; Auwärter, W.; Barth, J. V.; Palma, C.-A.; Müllen, K. Exploration of Pyrazine-Embedded Antiaromatic Polycyclic Hydrocarbons Generated by Solution and On-Surface Azomethine Ylide Homocoupling. *Nat. Commun.* **2017**, *8*, 1948.
(40) Feng, X.; Wu, J.; Ai, M.; Pisula, W.; Zhi, L.; Rabe, J. P.; Müllen, K. Triangle-Shaped Polycyclic Aromatic Hydrocarbons. *Angew. Chem., Int. Ed.* **2007**, *46*, 3033−3036.
(41) Liu, Y.; Marszalek, T.; Müllen, K.; Pisula, W.; Feng, X. Derivatizing Tribenzothiophene-Fused Hexa-Peri-Hexabenzocoronenes with Tunable Optoelectronic Properties. *Chem. - Asian J.* **2016**, *11*, 2107−2112.
(42) Martin, C. J.; Gil, B.; Perera, S. D.; Draper, S. M. Thienyl Directed Polyaromatic C−C Bond Fusions: S-Doped Hexabenzocoronenes. *Chem. Commun.* **2011**, *47*, 3616−3618.
(43) Tan, Y.-Z.; Yang, B.; Parvez, K.; Narita, A.; Osella, S.; Beljonne, D.; Feng, X.; Müllen, K. Atomically Precise Edge Chlorination of Nanographenes and Its Application in Graphene Nanoribbons. *Nat. Commun.* **2013**, *4*, 2646.
(44) Tan, Y.-Z.; Osella, S.; Liu, Y.; Yang, B.; Beljonne, D.; Feng, X.; Müllen, K. Sulfur-Annulated Hexa-Peri-Hexabenzocoronene Decorated with Phenylthio Groups at the Periphery. *Angew. Chem., Int. Ed.* **2015**, *54*, 2927−2931.
(45) Cao, J.; Liu, Y.-M.; Jing, X.; Yin, J.; Li, J.; Xu, B.; Tan, Y.-Z.; Zheng, N. Well-Defined Thiolated Nanographene as Hole-Transporting Material for Efficient and Stable Perovskite Solar Cells. *J. Am. Chem. Soc.* **2015**, *137*, 10914−10917.
(46) Wu, Z.-S.; Tan, Y.-Z.; Zheng, S.; Wang, S.; Parvez, K.; Qin, J.; Shi, X.; Sun, C.; Bao, X.; Feng, X.; Müllen, K. Bottom-Up Fabrication of Sulfur-Doped Graphene Films Derived from Sulfur-Annulated Nanographene for Ultrahigh Volumetric Capacitance Micro-Supercapacitors. *J. Am. Chem. Soc.* **2017**, *139*, 4506−4512.
(47) Xiao, S.; Myers, M.; Miao, Q.; Sanaur, S.; Pang, K.; Steigerwald, M. L.; Nuckolls, C. Molecular Wires from Contorted Aromatic Compounds. *Angew. Chem., Int. Ed.* **2005**, *44*, 7390−7394.
(48) Chiu, C.-Y.; Kim, B.; Gorodetsky, A. A.; Sattler, W.; Wei, S.; Sattler, A.; Steigerwald, M.; Nuckolls, C. Shape-Shifting in Contorted Dibenzotetrathienocoronenes. *Chem. Sci.* **2011**, *2*, 1480−1486.
(49) Chen, L.; Puniredd, S. R.; Tan, Y.-Z.; Baumgarten, M.; Zschieschang, U.; Enkelmann, V.; Pisula, W.; Feng, X.; Klauk, H.; Müllen, K. Hexathienocoronenes: Synthesis and Self-Organization. *J. Am. Chem. Soc.* **2012**, *134*, 17869−17872.
(50) Chen, L.; Mali, K. S.; Puniredd, S. R.; Baumgarten, M.; Parvez, K.; Pisula, W.; De Feyter, S.; Müllen, K. Assembly and Fiber Formation of a Gemini-Type Hexathienocoronene Amphiphile for Electrical Conduction. *J. Am. Chem. Soc.* **2013**, *135*, 13531−13537.
(51) Hill, J. P.; Jin, W.; Kosaka, A.; Fukushima, T.; Ichihara, H.; Shimomura, T.; Ito, K.; Hashizume, T.; Ishii, N.; Aida, T. Self-Assembled Hexa-Peri-Hexabenzocoronene Graphitic Nanotube. *Science* **2004**, *304*, 1481−1483.
(52) Sun, Z.; Ye, Q.; Chi, C.; Wu, J. Low Band Gap Polycyclic Hydrocarbons: from Closed-Shell Near Infrared Dyes and Semiconductors to Open-Shell Radicals. *Chem. Soc. Rev.* **2012**, *41*, 7857−7889.
(53) Ikeda, T.; Hou, Z.; Chai, G.-L.; Terakura, K. Possible Oxygen Reduction Reactions for Graphene Edges from First Principles. *J. Phys. Chem. C* **2014**, *118*, 17616−17625.
(54) Jiao, Y.; Zheng, Y.; Davey, K.; Qiao, S.-Z. Activity Origin and Catalyst Design Principles for Electrocatalytic Hydrogen Evolution on Heteroatom-Doped Graphene. *Nat. Energy* **2016**, *1*, 16130.
(55) Berger, R.; Giannakopoulos, A.; Ravat, P.; Wagner, M.; Beljonne, D.; Feng, X.; Müllen, K. Synthesis of Nitrogen-Doped ZigZag-Edge Peripheries: Dibenzo-9a-azaphenalene as Repeating Unit. *Angew. Chem., Int. Ed.* **2014**, *53*, 10520−10524.
(56) Berger, R.; Wagner, M.; Feng, X.; Müllen, K. Polycyclic Aromatic Azomethine Ylides: A Unique Entry to Extended Polycyclic Heteroaromatics. *Chem. Sci.* **2015**, *6*, 436−441.
(57) Ito, S.; Tokimaru, Y.; Nozaki, K. Isoquinolino[4,3,2-*de*]-phenanthridine: Synthesis and Its Use in 1,3-dipolar Cycloadditions to Form Nitrogen-Containing Polyaromatic Hydrocarbons. *Chem. Commun.* **2015**, *51*, 221−224.
(58) Ito, S.; Tokimaru, Y.; Nozaki, K. Benzene-Fused Azacorannulene Bearing an Internal Nitrogen Atom. *Angew. Chem., Int. Ed.* **2015**, *54*, 7256−7260.
(59) Tokimaru, Y.; Ito, S.; Nozaki, K. A Hybrid of Corannulene and Azacorannulene: Synthesis of a Highly Curved Nitrogen-Containing Buckybowl. *Angew. Chem., Int. Ed.* **2018**, *57*, 9818−9822.
(60) Wang, X.; Zhang, F.; Schellhammer, K. S.; Machata, P.; Ortmann, F.; Cuniberti, G.; Fu, Y.; Hunger, J.; Tang, R.; Popov, A. A.; Berger, R.; Müllen, K.; Feng, X. Synthesis of NBN-Type Zigzag-Edged Polycyclic Aromatic Hydrocarbons: 1,9-Diaza-9*a*-boraphenalene as a Structural Motif. *J. Am. Chem. Soc.* **2016**, *138*, 11606−11615.
(61) Liu, J.; Ravat, P.; Wagner, M.; Baumgarten, M.; Feng, X.; Müllen, K. Tetrabenzo[*a*,*f*,*j*,*o*]perylene: A Polycyclic Aromatic Hydrocarbon With an Open-Shell Singlet Biradical Ground State. *Angew. Chem., Int. Ed.* **2015**, *54*, 12442−12446.
(62) Liu, J.; Narita, A.; Osella, S.; Zhang, W.; Schollmeyer, D.; Beljonne, D.; Feng, X.; Müllen, K. Unexpected Scholl Reaction of 6,7,13,14-Tetraarylbenzo[*k*]tetraphene: Selective Formation of Five-

DOI: 10.1021/acs.accounts.9b00322
Acc. Chem. Res. 2019, 52, 2491−2505

Membered Rings in Polycyclic Aromatic Hydrocarbons. *J. Am. Chem. Soc.* **2016**, *138*, 2602−2608.
(63) Zöphel, L.; Berger, R.; Gao, P.; Enkelmann, V.; Baumgarten, M.; Wagner, M.; Müllen, K. Toward the Peri-Pentacene Framework. *Chem. - Eur. J.* **2013**, *19*, 17821−17826.
(64) Wang, X.-Y.; Narita, A.; Zhang, W.; Feng, X.; Müllen, K. Synthesis of Stable Nanographenes with OBO-Doped Zigzag Edges Based on Tandem Demethylation-Electrophilic Borylation. *J. Am. Chem. Soc.* **2016**, *138*, 9021−9024.
(65) Ajayakumar, M. R.; Fu, Y.; Ma, J.; Hennersdorf, F.; Komber, H.; Weigand, J. J.; Alfonsov, A.; Popov, A. A.; Berger, R.; Liu, J.; Müllen, K.; Feng, X. Toward Full Zigzag-Edged Nanographenes: Peri-Tetracene and Its Corresponding Circumanthracene. *J. Am. Chem. Soc.* **2018**, *140*, 6240−6244.
(66) Ni, Y.; Gopalakrishna, T. Y.; Phan, H.; Herng, T. S.; Wu, S.; Han, Y.; Ding, J.; Wu, J. A Peri-Tetracene Diradicaloid: Synthesis and Properties. *Angew. Chem., Int. Ed.* **2018**, *57*, 9697−9701.
(67) Katayama, T.; Nakatsuka, S.; Hirai, H.; Yasuda, N.; Kumar, J.; Kawai, T.; Hatakeyama, T. Two-Step Synthesis of Boron-Fused Double Helicenes. *J. Am. Chem. Soc.* **2016**, *138*, 5210−5213.
(68) Numano, M.; Nagami, N.; Nakatsuka, S.; Katayama, T.; Nakajima, K.; Tatsumi, S.; Yasuda, N.; Hatakeyama, T. Synthesis of Boronate-Based Benzo[*fg*]tetracene and Benzo[*hi*]hexacene via Demethylative Direct Borylation. *Chem. - Eur. J.* **2016**, *22*, 11574−11577.
(69) Wang, X.-Y.; Dienel, T.; Di Giovannantonio, M.; Barin, G. B.; Kharche, N.; Deniz, O.; Urgel, J. I.; Widmer, R.; Stolz, S.; De Lima, L. H.; Muntwiler, M.; Tommasini, M.; Meunier, V.; Ruffieux, P.; Feng, X.; Fasel, R.; Müllen, K.; Narita, A. Heteroatom-Doped Perihexacene from a Double Helicene Precursor: On-Surface Synthesis and Properties. *J. Am. Chem. Soc.* **2017**, *139*, 4671−4674.
(70) Wang, X.-Y.; Wang, X.-C.; Narita, A.; Wagner, M.; Cao, X.-Y.; Feng, X.; Müllen, K. Synthesis, Structure, and Chiroptical Properties of a Double [7]Heterohelicene. *J. Am. Chem. Soc.* **2016**, *138*, 12783−12786.
(71) Yao, X.; Zhang, K.; Müllen, K.; Wang, X.-Y. Direct C−H Borylation at the 2- and 2,7-Positions of Pyrene Leading to Brightly Blue- and Green-Emitting Chromophores. *Asian J. Org. Chem.* **2018**, *7*, 2233−2238.
(72) Cai, J.; Ruffieux, P.; Jaafar, R.; Bieri, M.; Braun, T.; Blankenburg, S.; Muoth, M.; Seitsonen, A. P.; Saleh, M.; Feng, X.; Müllen, K.; Fasel, R. Atomically Precise Bottom-Up Fabrication of Graphene Nanoribbons. *Nature* **2010**, *466*, 470−473.
(73) Bronner, C.; Stremlau, S.; Gille, M.; Braße, F.; Haase, A.; Hecht, S.; Tegeder, P. Aligning the Band Gap of Graphene Nanoribbons by Monomer Doping. *Angew. Chem., Int. Ed.* **2013**, *52*, 4422−4425.
(74) Zhang, Y.; Zhang, Y.; Li, G.; Lu, J.; Lin, X.; Du, S.; Berger, R.; Feng, X.; Müllen, K.; Gao, H.-J. Direct Visualization of Atomically Precise Nitrogen-doped Graphene Nanoribbons. *Appl. Phys. Lett.* **2014**, *105*, 023101.
(75) Cai, J.; Pignedoli, C. A.; Talirz, L.; Ruffieux, P.; Söde, H.; Liang, L.; Meunier, V.; Berger, R.; Li, R.; Feng, X.; Müllen, K.; Fasel, R. Graphene Nanoribbon Heterojunctions. *Nat. Nanotechnol.* **2014**, *9*, 896−900.
(76) Zhang, Y.-F.; Zhang, Y.; Li, G.; Lu, J.; Que, Y.; Chen, H.; Berger, R.; Feng, X.; Müllen, K.; Lin, X.; Zhang, Y.-Y.; Du, S.; Pantelides, S. T.; Gao, H.-J. Sulfur-Doped Graphene Nanoribbons with a Sequence of Distinct Band Gaps. *Nano Res.* **2017**, *10*, 3377−3384.
(77) Durr, R. A.; Haberer, D.; Lee, Y.-L.; Blackwell, R.; Kalayjian, A. M.; Marangoni, T.; Ihm, J.; Louie, S. G.; Fischer, F. R. Orbitally Matched Edge-Doping in Graphene Nanoribbons. *J. Am. Chem. Soc.* **2018**, *140*, 807−813.
(78) Wang, X.-Y.; Urgel, J. I.; Barin, G. B.; Eimre, K.; Di Giovannantonio, M.; Milani, A.; Tommasini, M.; Pignedoli, C. A.; Ruffieux, P.; Feng, X.; Fasel, R.; Müllen, K.; Narita, A. Bottom-Up Synthesis of Heteroatom-Doped Chiral Graphene Nanoribbons. *J. Am. Chem. Soc.* **2018**, *140*, 9104−9107.
(79) Talirz, L.; Ruffieux, P.; Fasel, R. On-Surface Synthesis of Atomically Precise Graphene Nanoribbons. *Adv. Mater.* **2016**, *28*, 6222−6231.
(80) de Oteyza, D. G.; García-Lekue, A.; Vilas-Varela, M.; Merino-Díez, N.; Carbonell-Sanromà, E.; Corso, M.; Vasseur, G.; Rogero, C.; Guitián, E.; Pascual, J. I.; Ortega, J. E.; Wakayama, Y.; Peña, D. Substrate-Independent Growth of Atomically Precise Chiral Graphene Nanoribbons. *ACS Nano* **2016**, *10*, 9000−9008.
(81) Kawai, S.; Nakatsuka, S.; Hatakeyama, T.; Pawlak, R.; Meier, T.; Tracey, J.; Meyer, E.; Foster, A. S. Multiple Heteroatom Substitution to Graphene Nanoribbon. *Sci. Adv.* **2018**, *4*, eaar7181.

DOI: 10.1021/acs.accounts.9b00322
Acc. Chem. Res. 2019, 52, 2491−2505